RSC Chemical Biology

ROYAL SOCIETY OF CHEMISTRY

PAPER

View Article Online
View Journal | View Issue

Cite this: *RSC Chem. Biol.*, 2026, 7, 729

Photoclickable Halotag ligands for spatiotemporal multiplexed protein labeling on living cells

Franziska Walterspiel, *† Begoña Ugarte-Uribe, Stefan Terjung, Alex Cabrera, Arif Ul Maula Khan and Claire Deo *

Precise spatiotemporal control over fluorescence labeling is a powerful approach for selective marking and tracking of proteins of interest within living systems. Here, we report a photoclickable labeling platform based on the 2,3-diaryl-indanone epoxide (DIO) photoswitch scaffold and the self-labeling protein HaloTag. Upon illumination, the protein-bound DIO undergoes reversible photoisomerization to form a metastable oxidopyrylium ylide (PY) that reacts with ring-strained dipolarophiles *via* [5 + 2] cycloaddition, enabling covalent spatiotemporal labeling. We synthesize and characterize a library of DIO-HaloTag and DIO-SNAP-tag ligands, systematically examining the effects of linker architecture and scaffold substitution on the photoswitching and photoclick reactivity *in vitro* and on living cells. We identify a naphthyl-substituted DIO ligand exhibiting superior photoswitching and photoclick efficiency, allowing fast, selective labeling of HaloTagged proteins on the surface of living cells using visible light activation (405 nm). Using this system, we achieve two- and three-color labeling of defined cell surface regions with excellent spatial and temporal precision, additionally allowing combinatorial labeling. Together, this work establishes a versatile framework for multiplexed, light-directed protein labeling compatible with living systems, with promising future applications including multiplexed long-term tracking and cellular barcoding.

Received 19th January 2026,
Accepted 2nd March 2026

DOI: 10.1039/d6cb00017g

rsc.li/rsc-chembio

Introduction

Precise spatiotemporal control of fluorescence is essential for dissecting complex biological processes in space and time, enabling selective marking and long-term tracking of proteins of interest within a biological sample.[1–3] This can be achieved using photo-responsive fluorophores, including light-controllable fluorescent proteins or small-molecule dyes,[4–7] targeted to proteins of interest. However, these unimolecular systems typically operate within a single spectral channel, restricting their utility to single color imaging. Extending photoactivation strategies to selectively label distinct protein subsets in different colors can offer a powerful method for long-term tracking and dynamic barcoding in complex biological environments. A particularly attractive strategy toward this goal is to control fluorophore conjugation photochemically, such that the labeling event itself is light-triggered.[8] In principle, this can enable repeated labeling cycles with different fluorophores, yielding highly multiplexed and programmable fluorescent tagging of cellular protein targets. Several approaches have been explored using photoresponsive systems, including host–guest pairs,[9] photocaged self-labeling tags or ligands,[10,11] and photoclick reactions.[12–16] Despite these advances, achieving multicolor and spatiotemporally resolved protein labeling at the subcellular level remains challenging. Indeed, the activated species must remain localized to prevent off-target labeling by diffusion, and must either fully react or deactivate rapidly after reaction to allow sequential re-labeling. To date, only a few systems have demonstrated true sequential multicolor labeling,[9,16] and broadly applicable, subcellular-scale approaches compatible with live-cell imaging are still lacking.

Here, we present a photoclickable labeling system based on the self-labeling protein HaloTag,[17,18] enabling sequential multicolor labeling of proteins on the surface of living cells with excellent spatiotemporal control using visible light (Fig. 1a). Our design is based on the 2,3-diaryl-indanone epoxide (DIO) scaffold, which undergoes reversible photoisomerization to form a metastable oxidopyrylium ylide (PY) intermediate.[19,20] The PY species can spontaneously react *via* [5+2] cycloaddition with ring-strained dipolarophiles such as bicyclononyne (BCN) and *trans*-cyclooctene (TCO) (Fig. 1b).[21] This reactivity was recently exploited for single-color fluorescence labeling on live-cell surfaces *via* antibody conjugation.[20] We reasoned that integrating this photoswitchable–photoclickable platform with a broadly applicable self-labeling protein tag could yield a robust and generalizable strategy for photo-controlled protein labeling compatible with living systems. For this purpose, we rationally design and synthesize a small library of DIO-ligands

European Molecular Biology Laboratory, Meyerhofstraße 1, 69117 Heidelberg, Germany. E-mail: claire.deo@embl.de, franziska.walterspiel@embl.de
† Present address: Max Planck Institute for Medical Research, Heidelberg, Germany.

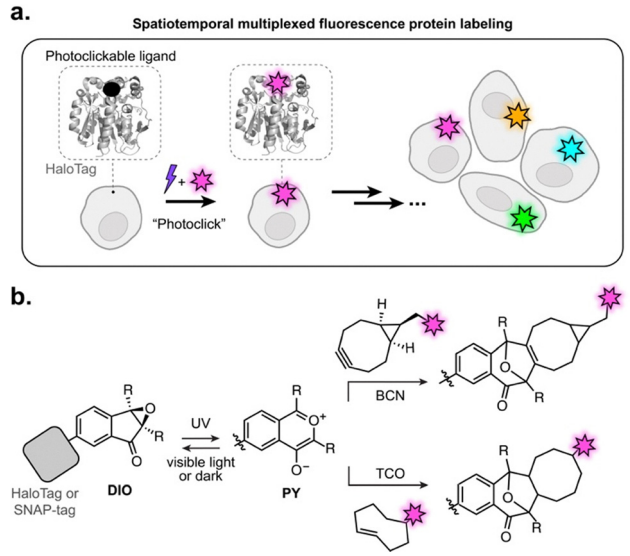

Fig. 1 (a) General approach for spatiotemporal multiplexed fluorescence protein labeling using photoclickable HaloTag ligands. (b) Photoswitching and subsequent click reaction of protein-bound DIO with bicyclononyne (BCN) or *trans*-cyclooctene (TCO) attached to fluorophores, to yield fluorescently labeled proteins.

of the self-labeling HaloTag[17,18] and SNAP-tag,[22] and systematically investigate their reactivity *in vitro* and on the surface of living cells. We develop a naphthyl-substituted DIO ligand which undergoes efficient photoclick reaction with fluorophores on HaloTag, in only a few seconds of illumination with visible light (405 nm). With this novel system, we achieve multicolor labeling of specifically targeted regions on living cell surface, both at the cellular and subcellular level. To the best of our knowledge, this is the first example of such controlled multicolor marking on a single cell, opening promising applications for dynamic imaging of cells or cell surface protein targets.

Results and discussion

Design and synthesis

To engineer a system for generalizable photo-controlled protein labeling, we set out to adapt the DIO-PY photoclickable scaffold to the well-established self-labeling protein tags HaloTag[17,18] and SNAP-tag.[22] In particular, we reasoned that the mode of attachment to the protein would be critical for function. Indeed, the tight interaction of the protein tag with its ligand is known to substantially alter the local environment around the substrate,[23] which in this instance could potentially impair photoswitching and/or subsequent click reaction. We therefore examined both HaloTag and SNAP-tag systems, and designed a small library of DIO ligands (Fig. 2a and Fig. S1). We started with the simplest, unsubstituted, DIO scaffold, functionalized at the 6-position of the indanone core with the respective protein tag ligand. For HaloTag, we assessed the influence of linker length (compounds **1–3**) and rigidity (compound **10**). For SNAP-tag, we compared the conventional benzyl-guanine (compound **4**) and benzyl-chloropyrimidine (compound **5**) ligands.[24] In addition, substitution on the phenyl rings at the 2,3-position of the DIO scaffold has been shown to substantially affect their properties,[20] and we therefore also included sterically hindered derivatives (naphthyl analogs **6** and **7**), and compounds bearing electron-withdrawing substituents (CF_3 derivatives **8** and **9**), to fine-tune reactivity. The 6-carboxy DIO derivatives were synthesized *via* a palladium-catalyzed annulation from the corresponding 1,2-diphenylethynes, followed by epoxidation (Fig. S2–S6). The resulting functionalized DIO intermediates were then subjected to amide coupling with the NH_2-substituted ligands to afford compounds **1–10**.

Photophysical properties *in vitro*

This new library of DIO-based ligands was characterized *in vitro*. The DIO → PY photoswitching was induced by illumination at 375 nm (700 μW cm^{-2}), using a custom-built LED device (Fig. S7).[25] In the dark, the free ligands **1–10** showed no absorption in the visible range, consistent with the chemical structure of the DIO scaffold (Fig. S8). Illumination at 375 nm in a PBS : MeCN (1 : 1) mixture led to formation of the reactive PY species, evidenced by an increase in absorption in both the UV (350–400 nm, π → π* transition) and visible regions (450–650 nm, n → π* transition). Importantly, formation of the PY isomer was fully reversible upon illumination at 545 nm (700 μW cm^{-2}), indicating efficient back-isomerization to the initial state, and allowing multiple 375 nm/545 nm switching cycles with minimal loss in performance, except for compounds **6**, **8** and **9** which showed lower fatigue resistance (Fig. S9). The DIO → PY photoconversion was also thermally reversible in the dark, with half-lives ($t_{1/2,relax}$) ranging from 15 to 200 min for the free ligands at room temperature, in the same range as previously reported (Fig. S9 and Table S1).[20] Compounds **1–5** displayed comparable photoswitching amplitude and kinetics (ε between 600 and 2200 M^{-1} cm^{-1} at the photostationary state (PSS), $t_{1/2,relax}$ between 60 and 87 min^{-1}, Table S1), indicating that the ligand itself does not significantly affect photoswitching. Compounds **6** and **7** were red-shifted by 20 nm, and exhibited substantially higher absorption at the PSS (ε = 10 000 and 5400 M^{-1} cm^{-1}, respectively), while relaxation kinetics were similar to compounds **1–5**. Introduction of CF_3 substituents on the phenyl rings (**8**,**9**) accelerated thermal relaxation,[20] while, in contrast, compound **10** showed markedly slower relaxation. In aqueous buffer alone, all ligands exhibited substantial aggregation (Fig. S10); however, light-induced formation and disappearance of the ~520 nm absorption band confirmed that photoswitching still occurred under these conditions. Only free ligand **7** did not display measurable photoswitching behavior in aqueous buffer, possibly due to aggregation due to the combination of hydrophobic naphthyl groups and the long HaloTag ligand.

Next, we evaluated the properties of ligands **1–10** covalently bound to their respective self-labeling protein tags in solution. Binding efficiency to the purified proteins was assessed *via* pulse-chase assay with JF_{635}-HaloTag or -SNAP-tag ligands (Fig. S11).[26] All ligands except **5** achieved >90% protein labeling within two hours, and in all cases complete labeling was obtained after five hours at room temperature. Importantly, all

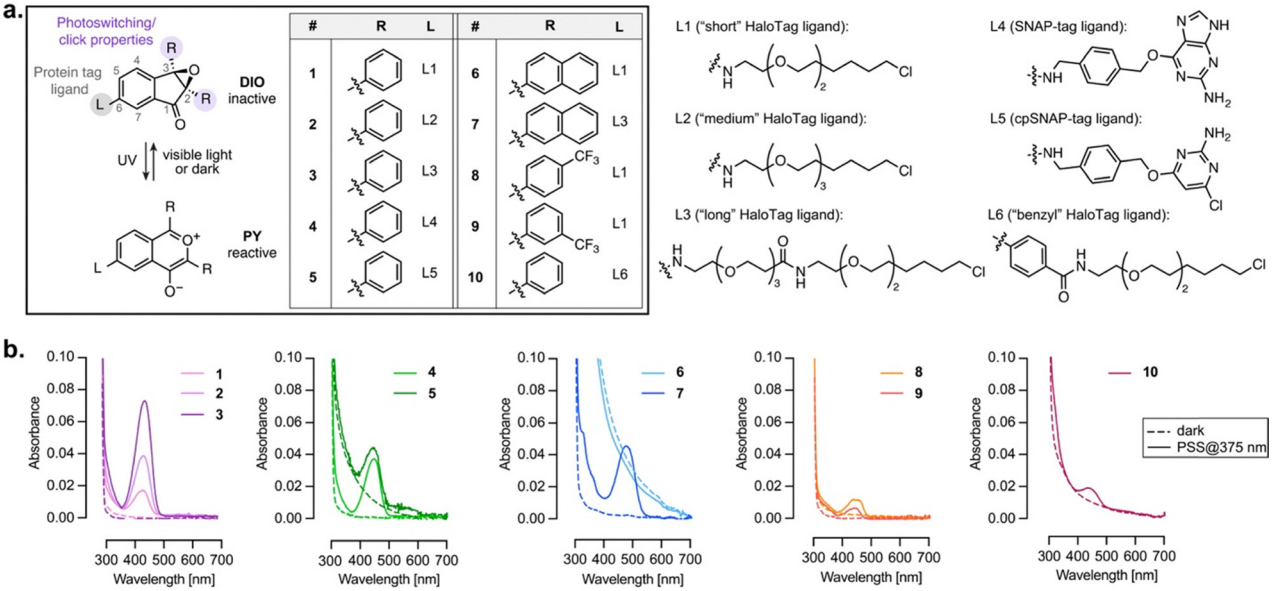

Fig. 2 (a) Chemical structures and photoswitching of DIO ligands **1–10** synthesized and studied in this work. (b) Absorption spectra of ligands **1–10** bound to HaloTag or SNAP-tag in the dark (dashed lines), and at the photostationary state (PSS) reached after illumination at 375 nm (solid lines).

protein-bound ligands except **6** retained photoswitching, as evidenced by the increase in visible absorption upon illumination at 375 nm (Fig. 2b and Fig. S12). Surprisingly however, all bound ligands displayed an ~80 nm blue shift of the visible absorption (λ_{max} = 437–474 nm) compared to the free compounds, suggesting that the PY isomer interacts closely with the protein surface. The protein-bound PY isomers exhibited weak fluorescence (λ_{em} = 474–537 nm, $\Phi_F \leq 0.24$, Fig. S13). Photoswitching amplitude varied markedly across protein–ligands conjugates (Fig. 2b and Fig. S12): more efficient switching was observed with increasing linker length (*e.g.* **3** > **2** > **1**), evidenced by larger absorption at the photostationary state. In contrast, the rigid spacer in **10** resulted in a lower turn-on. SNAP-tag ligands **4** and **5** displayed photoswitching amplitude comparable to compound **2**, likely reflecting the greater conformational flexibility of the SNAP-tag surface.[22] Within the naphthyl series, compound **6** exhibited negligible switching, likely due to its poor binding to HaloTag, whereas **7** showed large absorption increase. CF_3-substituted compounds **8,9** displayed smaller photo-responses. Overall, the protein-bound ligands exhibited slower photoswitching kinetics compared to the free ligands (Table S2), and did not display thermal relaxation over two hours (Fig. S14), further evidencing the strong impact of the protein scaffold on the photoswitching properties. Nevertheless, the photoisomerization was reversible upon illumination at 450 nm (Fig. S12). Overall, the similar behavior observed regardless of ligand linker length, and for both HaloTag and SNAP-tag, supports a non-residue-specific effect stemming from the interaction with the protein, which could potentially arise from local pH, polarity or electrostatics around the protein surface. We investigated this using either ligand **7** (as the best performing compound, *vide infra*), or the simplest ligand **1** (Fig. S15–S18). Varying the pH in the range 4–9 did not elicit any shift in absorption spectrum for either the free ligand (Fig. S15) or the protein-bound ligand (Fig. S16), allowing to exclude protonation effects. Varying solvent polarity did also not result in any shift in absorption spectrum of the PY species (Fig. S17). Finally, we examined the photoswitching of free ligand **7** in the presence of bovine serum albumin (Fig. S18). In this instance, illumination at 375 nm led to formation of the ~450 nm absorption peak, similarly as with HaloTag and SNAP-tag. Overall, the behavior of the PY isomer on protein is highly reminiscent of the behavior of rhodamine derivatives,[27] which displays a shift in equilibrium between two isomers upon interaction with a variety of protein partners. This suggests that the PY form could exist in equilibrium between two forms, one absorbing around 550 nm and strongly favored in solution, and one absorbing ~450 nm, long-lived and stabilized on protein surfaces, while retaining photo-responsive behavior.

As increasing linker length did not abolish the protein–switch interaction, we next examined whether altering the protein structure itself could eliminate this interaction, hence restoring photoswitching behavior similar to that of the free ligand. Our previous study showed that HaloTag circularly permuted at position 178 (cp178HaloTag) retained binding to JF_{635}-HaloTag ligand without fluorescence turn-on, evidencing minimal interaction with the bound fluorophore.[25] We therefore investigated the photoswitching of compound **7** with cp178HaloTag (Fig. S19). Compound **7** efficiently bound to the modified protein (Fig. S19b). Upon illumination at 375 nm, photoswitching occurred, yielding two absorption bands at 460 and 561 nm, therefore partially recovering the red-shifted absorption characteristic of the free ligand. This isomerization was somewhat reversible upon illumination at 545 nm, which suggests that the reduced interaction with cp178HaloTag partially restores free-ligand-like photoswitching

behavior. Overall, all compounds except compound 6 exhibited reversible photoswitching upon 375 nm/450 nm illumination when bound to HaloTag or SNAP-tag, and we next examined their potential as photoclickable protein-labeling partners.

Photoclick reaction *in vitro*

The metastable PY species formed upon illumination has been shown to undergo spontaneous [5+2] cycloaddition with bicyclononyne (BCN) and *trans*-cyclooctene (TCO) derivatives, yielding a covalent adduct under physiological conditions (Fig. 1b).[20] To assess whether our protein-bound system retained similar reactivity, we illuminated the DIO–protein tag conjugates in the absence or presence of *endo*-BCN, in aqueous buffer (Fig. S20). In the absence of *endo*-BCN, photoswitching proceeded as described above, evidenced by the gradual increase in visible absorption around 440 nm. In contrast, no absorption increase was observed in the presence of *endo*-BCN. This indicates that the species formed upon illumination rapidly reacts with *endo*-BCN to form the non-absorbing covalent adduct, supporting that all the DIO–protein conjugates undergo efficient photoclick reaction under physiological conditions. Interestingly, when excess *endo*-BCN was added only after illumination (once the photostationary state had been reached), the visible absorption showed only minor decrease, suggesting very slow click reaction under these conditions (Fig. S21a and b). The free ligand did not show this behavior, undergoing rapid reaction with *endo*-BCN regardless of illumination/addition order (Fig. S21c and d). These observations suggest that the species reactive toward the click reaction on protein is not the long-lived form absorbing around 440 nm, but rather a transient intermediate generated during the photoswitching process, which could likely be the 550 nm absorbing PY species visible in free ligand solution.

To further evaluate the possibility to use the photoclick reaction for fluorescence protein labeling, we synthesized clickable fluorophore **11** (JF_{549}-BCN, Fig. 3a and Fig. S22–S24), and examined its [5+2] cycloaddition with protein-bound ligands **1–10** by SDS-PAGE gel electrophoresis (Fig. 3b and e). The DIO–protein conjugates were incubated with excess JF_{549}–BCN and either kept in the dark or illuminated (375 nm, 700 μW cm^{-2}, 10 min). After removal of unreacted dye and denaturation, gel electrophoresis clearly revealed light-dependent fluorescence labeling. For all HaloTag ligands (**1–3**, **6–10**), the click reaction was highly efficient, fully saturating the HaloTag as evidenced by the positive control for maximal intensity JF_{549}-HaloTag ligand ($Halo_{549}$, Fig. 3b).[26] On a side note, compound **6** (which did not show measurable photoswitching on protein, see Fig. S12) surprisingly showed efficient photoclick reaction, which suggests that it still undergoes photoswitching but with a switching amplitude or thermal relaxation rate making it non measurable under our conditions. Ligands **6** and **7** exhibited minor residual labeling in the dark, likely due to their red-shifted absorption spectra which render them more sensitive to residual ambient light during handling. In contrast, SNAP-tag ligands **4** and **5** displayed reduced photoclick efficiency, reaching only 40–50% labeling under identical conditions. As protein-bound **4** and **5** exhibited similar photoswitching as **2** (Fig. 2b), this significant difference can be attributed solely to the protein scaffold, with the SNAP-tag environment partly impairing the photoclick reaction. Kinetic analysis of **3**-HaloTag revealed that the reaction reached >80% completion within 5 min under our illumination conditions, and that equimolar amount of JF_{549}-BCN was sufficient for complete reaction (Fig. S25a–d). Light-intensity titration indicated that photoswitching, rather than cycloaddition, was the rate-limiting step (Fig. S25e and f). Overall, these results demonstrate that the

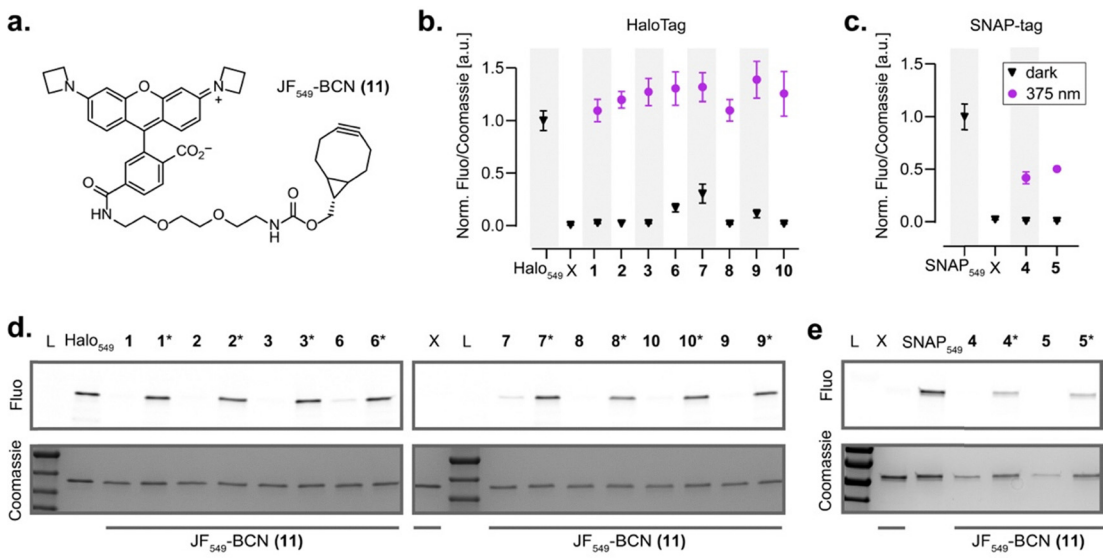

Fig. 3 Photoclick reaction with protein-bound **1–10** *in vitro*. (a) Structure of JF_{549}-BCN **11**. (b) and (c) Normalized JF_{549} fluorescence/Coomassie signal ratio in the dark (black triangles) and after photoclick reaction (purple dots) for protein-bound ligand **1–10**, quantified on the corresponding SDS-PAGE gels in (d) and (e) mean ± SEM for three replicates. HaloTag and SNAP-tag labeled with the corresponding JF_{549} ligand ($Halo_{549}$ and $SNAP_{549}$, respectively) were used as positive control for maximal labeling. X: no ligand; L: protein ladder. * In (d) and (e) indicates the illuminated samples, the other samples were kept in the dark.

photoclick reaction proceeds efficiently for protein-bound ligands *in vitro*, leading to controlled fluorescence protein labeling, with the HaloTag conjugates showing the highest reactivity.

Photo-controlled protein labeling on the surface of living cells

We next evaluated the use of ligands **1–10** with living cells, first by assessing protein labeling efficiency inside cells. SNAP-tag–HaloTag was expressed in the cytosol and, similarly as *in vitro*, the labeling efficiency was determined by pulse–chase assay using JF_{635}-HaloTag ligand or JF_{635}-SNAP-tag ligand to quantify remaining unbound protein after incubation with ligands **1–10** (Fig. S26–S28, see Methods). Ligands **1**, **3**, **7**, **9**, **10** showed >75% labeling after two hours, whereas **2**, **6** and **8** produced somewhat weaker labeling (40–65%). SNAP-tag ligands **4** and **5** showed negligible labeling in these conditions, possibly due to lower membrane permeability.

Next, we investigated the photoclick reaction, first on the surface of living cells. Living U2OS cells co-expressing a SNAP-tag–HaloTag fusion on the cell surface (targeted to PDGFR cell surface receptor) and EGFP in the cytosol were first labeled with DIO ligands **1–10**. For the clickable fluorophore, we used the commercially available, cell-impermeant CF®647-TCO, as TCO compounds were also show to undergo photoclick reaction with the DIO-PY scaffold in cellular experiments.[20] The clickable fluorophore was added to the medium before the plates were either illuminated at 375 nm for 5 min, or kept in the dark (Fig. 4a).

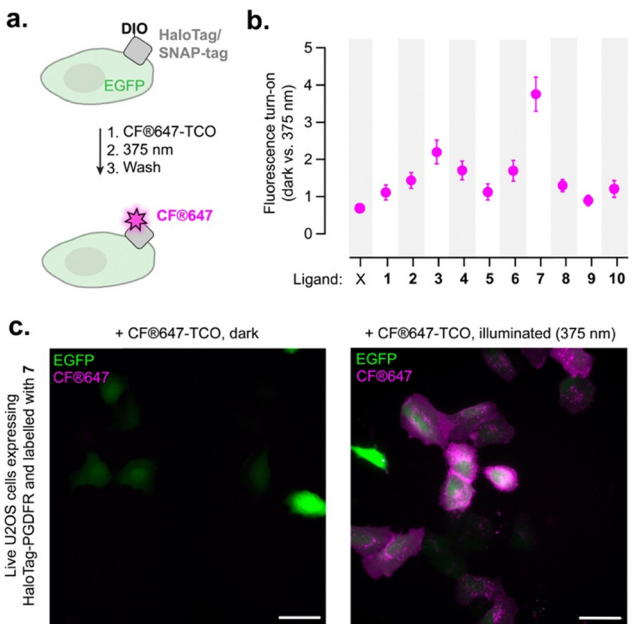

Fig. 4 (a) Photoclick labeling with CF®647-TCO on living U2OS cells co-expressing cell surface SNAP-tag–HaloTag fusion and cytosolic EGFP. (b) Fluorescence turn-on of cells labeled with ligands **1–10** or no ligand (X) after photoclick reaction with CF®647-TCO (2 μM) induced by illumination at 375 nm for 5 minutes (700 μW cm^{-2}). Mean ± SEM for $N > 200$ cells in each condition, two independent replicates. (c) Representative widefield fluorescence images for compound **7** incubated with CF®647-TCO and kept in the dark (left panel) and after photoclick reaction (right panel). Scale bars: 50 μm.

Excess fluorophore was washed away, and click efficiency was quantified by widefield fluorescence microscopy (Fig. 4b, c and Fig. S29–S32). While most ligands led to only a modest increase in far-red fluorescence following illumination, ligand **7** exhibited the highest performance, yielding ~4-fold increase in far-red fluorescence intensity after photoclick reaction, with fluorescence signal localized on the cell surface, consistent with protein-targeted photoclick labeling (Fig. 4c and Fig. S30). Flow cytometry confirmed these findings, showing ~3-fold higher fluorescence signal for **7** compared to the other ligands (Fig. S33 and S34). Unfortunately, the photoclick experiment was unsuccessful when HaloTag was expressed intracellularly (see Supplementary Note and Fig. S40–S42). Although specific labeling was detected in HaloTag-expressing cells, the signal was weak and accompanied by non-specific fluorescence in subcellular compartments. The photoswitching behavior observed for protein-bound compounds is likely responsible for the poor intracellular reactivity. Indeed, efficient click labeling requires the clickable fluorophore to be present locally during the photoswitching event (Fig. S21), a condition that may not met in the crowded intracellular environment where fluorophore availability may be limited. Altogether, these results underscore that further engineering will be required to improve the performance of this first-generation system in living cells.

As ligand **7** displays comparable performance to the other HaloTag ligands *in vitro* (both in terms of protein labeling and photoclick reactivity), the basis for its markedly enhanced activity on the surface of living cells remains unclear. This discrepancy may arise from subtle differences in photoswitching properties, including photoisomerization quantum yield or photostationary state composition, or from differences in click reaction kinetics that are not captured under our *in vitro* assay conditions. Importantly, these parameters are difficult to quantify for protein-bound compounds. Generally, this observation reflects the important differences between cellular environments and simplified *in vitro* systems, highlighting the necessity of systematic evaluation in live-cell contexts to identify suitable tools. Overall, ligand **7** clearly outperformed all other compounds, enabling efficient, selective, and non-toxic (Fig. S35) photoclick labeling of HaloTag protein fusions on the surface of living cells.

The efficient photoclick reaction on HaloTag can enable selective, sequential labeling of HaloTag-expressing cells or cell-surface regions with distinct colors defined by targeted illuminated areas, thereby allowing fluorescence barcoding of spatially and temporally defined targets. This approach, however, requires that all reactive species formed during labeling with the first color are fully inactivated before introducing the second color, to prevent signal leakage into undesired regions. The DIO-PY system was only previously used in single color labeling.[20] However, its thermal and photochemical reversibility makes it particularly well suited for sequential multicolor photolabeling. We therefore evaluated the best-performing ligand **7** for two-color surface labeling of living cells (Fig. 5a and Fig. S36). Living U2OS cells co-expressing cell surface HaloTag and intracellular EGFP were labeled with ligand **7**. CF®647–TCO was

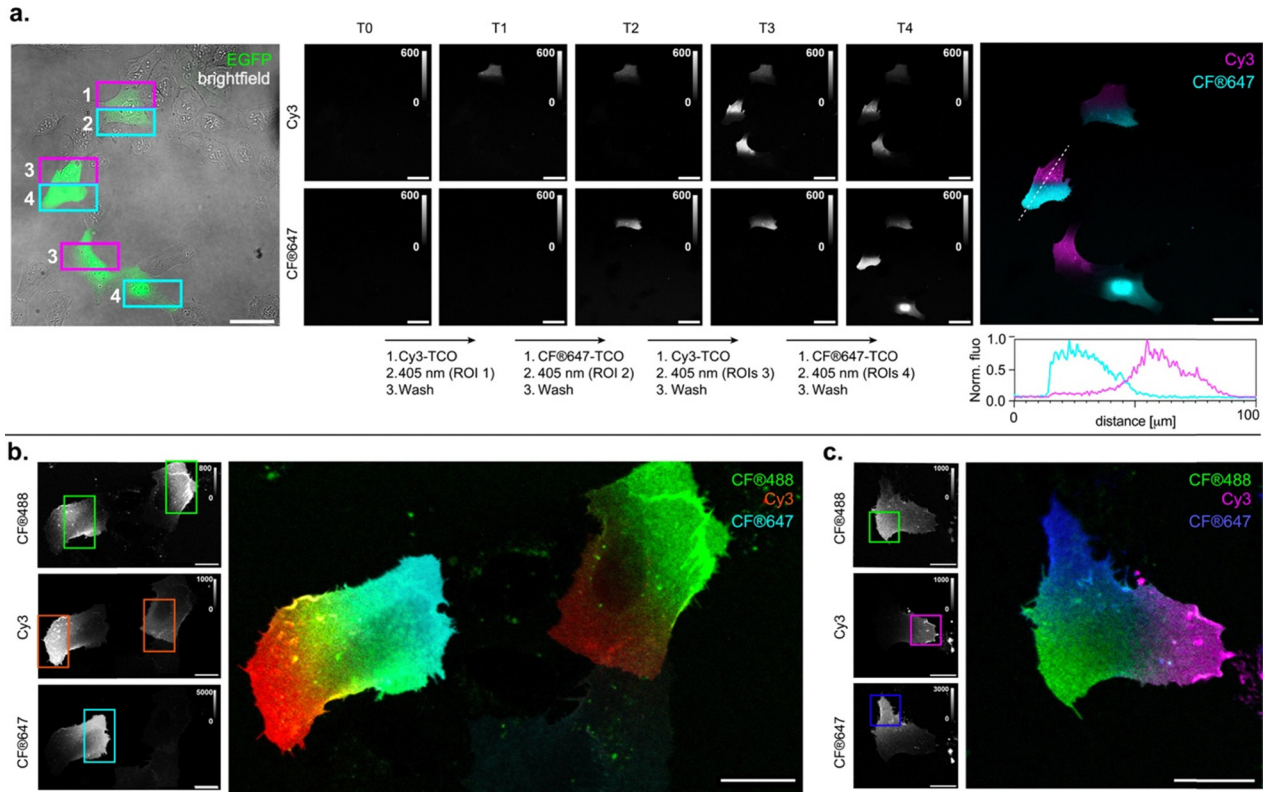

Fig. 5 Spatiotemporal multicolor labeling of living U2OS cells expressing extracellular SNAP-tag–HaloTag fusion and labeled with ligand **7**. (a) Confocal images of two-color sequential labeling. Illumination of selected ROIs was performed at 405 nm for 20 s (T1–T4) in the presence of CF®647-TCO or Cy3-TCO (2 µM) (see Methods). From left to right: fluorescence in EGFP channel with selected ROIs for the four successive cycles; fluorescence images for the Cy3 (middle top) and CF®647 (middle bottom) channels, after each photoclick cycle; overlay of the Cy3 and CF®647 channels after final cycle, with line profile quantification underneath. Representative images of five independent experiments. Scale bars: 50 µm. (b) and (c) Confocal images of the result of a three-color sequential labeling with CF®488A-TCO, Cy3-TCO and CF®647-TCO, with illuminated ROIs in each round indicated in the respective channel. Representative images of three independent experiments. Scale bars: 20 µm.

added to the medium, and selected cell regions were illuminated for 20 seconds using the confocal laser scanning microscope. Interestingly, the small spectral red-shift observed for compound 7 enabled activation to be performed with visible light at 405 nm (scanning speed, 4 µs per pixel, 41 kW cm^{-2}, see Methods). After washing away excess dye using a microfluidics system, the photoclick process was repeated with the blue-shifted Cy3–TCO, illuminating different cellular regions. Gratifyingly, spatially defined and highly selective two-color labeling was clearly visible, with no detectable signal in non-illuminated regions. This indicates that external deactivation of potentially remaining reactive species is not necessary between cycles, greatly simplifying the workflow. This could be a direct consequence of the photoswitching behavior observed for the protein-bound ligands (*vide supra*), showing that the species reactive towards the click reaction is only transiently formed upon illumination before formation of a thermally stable, non-reactive species. Importantly, only a few seconds of illumination are required to achieve clearly visible labeling. The resulting fluorescence labeling was stable over time, and imaging over time clearly shows motion of labeled surface proteins (Fig. S37 and Movie S1). By using cells not expressing EGFP, this strategy could be readily extended to three-color labeling, even within a single cell, demonstrating the versatility and precision of fluorescence labeling in defined subcellular regions (Fig. 5b, c and Fig. S38). Ultimately, the number of accessible unique fluorescence identifiers is limited by the multiplexing capability of the microscope. However, multiple fluorescence barcodes can still be generated using only a small number of fluorophores by performing combinatorial labeling. In practice, the labeling can be precisely controlled simply by adjusting the degree of photoactivation, defined by the microscope illumination time/power. Using this approach, we demonstrate that four cells can be distinctively labeled using only two fluorophores in two photoclick cycles (Fig. S39). Quantifiable labeling could be achieved with as little as 5 seconds of illumination. This combinatorial labeling could be quantified, with the ratio of signal intensity in the two channels showing good correlation with illumination time (Fig. S39c). Although this optical barcoding strategy using a limited set of fluorophores will require system-specific calibration, these results demonstrate the proof-of-principle for highly multiplexed fluorescence barcoding of HaloTagged protein targets on the surface of living cells.

Conclusion

In conclusion, we synthesized and systematically characterized a family of DIO-based photoclickable ligands for self-labeling protein tags, enabling light-controlled protein labeling under physiological conditions. Through systematic variation of linker length, rigidity, and protein tag partner, we established structure–property relationships governing photoswitching efficiency and photoclick reactivity, and evidence the strong influence of the protein environment on these properties. Among this family of ligands, the novel naphthyl-DIO ligand 7 emerged as the most efficient, showing robust light-induced labeling of HaloTag protein fusions on the surface of living cell. We demonstrate that this system enables highly specific, multicolor labeling of spatially and temporally defined cells and cell surface regions. The short illumination time required and the spontaneous deactivation of the reactive intermediate enable a rapid and streamlined labeling workflow, establishing this system as a practical tool for fluorescence barcoding.

Unfortunately, this first-generation tool did not show suitable performance inside living cells. Achieving intracellular protein labeling will require further investigation of the photoswitching mechanism, and optimization of the system, which could be achieved through structural modifications of the photoswitch scaffold, as well as protein engineering on the self-labeling tag. Nevertheless, the current iteration already enables precise labeling on the cell surface, and, to the best of our knowledge, constitutes first example of multicolor protein labeling at the subcellular scale. This already opens promising applications for multiplexed cell or cell-surface protein tracking on live samples, such as distinctly marking several subsets of cell-surface proteins to visualize how they rearrange during cell division, or distinctly marking multiple cells within a sample to follow their fate/migration over time. Additionally, this platform could be readily applied to other clickable fluorescent partners including functional reporters such as biosensors, and extended to non-optical applications such as affinity capture handles or oligonucleotides barcodes.[28,29] Together, these results demonstrate that tailoring the DIO-PY system to the self-labeling HaloTag enables robust spatiotemporally controlled protein labeling on living cells, hereby expanding the toolbox for light-directed multiplexed protein tagging.

Author contributions

FW: conceptualization, investigation, methodology, formal analysis, validation, visualization, writing (original draft, review & editing); BUU: investigation, methodology, writing (review & editing); ST: investigation, methodology, writing (review & editing); AC: investigation, methodology, writing (review & editing); AUMK: software, data curation, writing (review & editing); CD: funding acquisition, project administration, resources, supervision, formal analysis, visualization, writing (original draft, review & editing).

Conflicts of interest

The authors declare no competing interests.

Abbreviations

BCN	Bicyclononyne
DIO	2,3-Diaryl-indanone epoxide
HTL	HaloTag ligand
PSS	Photostationary state
PY	Oxidopyrylium ylide
STL	SNAP-tag ligand
TCO	*trans*-Cyclooctene.

Data availability

Supplementary information (SI): supplementary figures and tables, methods, synthesis and characterization for all new compounds (pdf). Movie S1: time-lapse of two-color sequential fluorescence labeling on targeted regions of living cell surface. See DOI: https://doi.org/10.1039/d6cb00017g.

The image analysis code used for segmentation and intensity quantification of widefield images was adapted from previous work.[25] It can be found along with test data at https://git.embl.org/grp-cba/htlov-mitochondria-intensity-quantification.

Acknowledgements

This work was supported by the European Molecular Biology Laboratory (EMBL) and the Chan Zuckerberg Initiative (Deep Tissue Imaging grant no. 2024-337799). The authors acknowledge: the Lavis group (Janelia Research Campus, HHMI) for sharing fluorophores; the Johnsson group (MPI for Medical Research) for sharing plasmids; Franziska Kundel and Marina Makharova (EMBL) for help with the microfluidics system; The Core Facilities at EMBL: the Electrical and Mechanical Workshops (LED illumination device), the Protein Expression and Purification Core Facility (protein purification and characterization), the Advanced Light Microscopy Facility (live cell imaging), the Bioimage Analysis Service team of EMBL Data Science Centre (image analysis), the Flow Cytometry Core Facility (flow cytometry data acquisition and analysis), the Metabolomics Core Facility (liquid chromatography-mass spectrometry data acquisition and analysis).

References

1 J. M. Kebschull and A. M. Zador, Cellular barcoding: lineage tracing, screening and beyond, *Nat. Methods*, 2018, **15**(11), 871–879, DOI: 10.1038/s41592-018-0185-x.
2 D. L. Coutu and T. Schroeder, Probing cellular processes by long-term live imaging–historic problems and current solutions, *J. Cell Sci.*, 2013, **126**(Pt 17), 3805–3815, DOI: 10.1242/jcs.118349.
3 S. Skylaki, O. Hilsenbeck and T. Schroeder, Challenges in long-term imaging and quantification of single-cell dynamics, *Nat. Biotechnol.*, 2016, **34**(11), 1137–1144, DOI: 10.1038/nbt.3713.
4 F. M. Jradi and L. D. Lavis, Chemistry of Photosensitive Fluorophores for Single-Molecule Localization Microscopy, *ACS Chem. Biol.*, 2019, **14**(6), 1077–1090, DOI: 10.1021/acschembio.9b00197.

5 R. Heinrich, W. Hussein and S. Berlin, Photo-transformable genetically-encoded optical probes for functional highlighting in vivo, *J. Neurosci. Methods*, 2021, **355**, 109129, DOI: 10.1016/j.jneumeth.2021.109129.
6 M. Olesinska-Monch and C. Deo, Small-molecule photoswitches for fluorescence bioimaging: engineering and applications, *Chem. Commun.*, 2023, **59**(6), 660–669, DOI: 10.1039/d2cc05870g.
7 R. Nifosì, B. Storti and R. Bizzarri, Reversibly switchable fluorescent proteins: "the fair switch project", *La Riv. Nuovo Cimento*, 2024, **47**(2), 91–178, DOI: 10.1007/s40766-024-00052-1.
8 Y. Miao, Y. Tian and D. Ye, Activatable covalent labeling probes: design, mechanism, and biological applications, *Chem. Soc. Rev.*, 2025, **54**, 11624–11658, DOI: 10.1039/d5cs00984g.
9 A. Som, M. Pahwa, S. Bawari, N. D. Saha, R. Sasmal, M. S. Bosco, J. Mondal and S. S. Agasti, Multiplexed optical barcoding of cells *via* photochemical programming of bioorthogonal host-guest recognition, *Chem. Sci.*, 2021, **12**(15), 5484–5494, DOI: 10.1039/d0sc06860h.
10 P. Mauker, C. B. J. Zecha, L. Dessen-Weissenhorn, L. Román-Albasini, J. C. M. Meiring, J. I. Brandmeier, D. Beckmann, J. P. Prohaska, M. Reynders, Y. L. Li, *et al.*, Logic-gating the HaloTag system with Conditional-Halo-ligator 'CHalo' reagents, *bioRxiv*, 2025, preprint, DOI: 10.1101/2025.09.23.676741.
11 S. Mandl, B. Maiwald, E. Adlmanninger, R. Birke, S. Schlee, A. Pruska, P. Bittner, R. Zenobi, T. Soykan and G. Beliu, *et al.*, SNAPpa: A Photoactivatable SNAP-tag for the Spatiotemporal Control of Protein Labeling, *JACS Au*, 2025, **5**(7), 3589–3602, DOI: 10.1021/jacsau.5c00603.
12 A. Jemas, Y. Xie, J. E. Pigga, J. L. Caplan, C. W. Am Ende and J. M. Fox, Catalytic Activation of Bioorthogonal Chemistry with Light (CABL) Enables Rapid, Spatiotemporally Controlled Labeling and No-Wash, Subcellular 3D-Patterning in Live Cells Using Long Wavelength Light, *J. Am. Chem. Soc.*, 2022, **144**(4), 1647–1662, DOI: 10.1021/jacs.1c10390.
13 A. D. Guo, D. Wei, H. J. Nie, H. Hu, C. Peng, S. T. Li, K. N. Yan, B. S. Zhou, L. Feng and C. Fang, *et al.*, Light-induced primary amines and o-nitrobenzyl alcohols cyclization as a versatile photoclick reaction for modular conjugation, *Nat. Commun.*, 2020, **11**(1), 5472, DOI: 10.1038/s41467-020-19274-y.
14 F. Wang, H. Kong, X. Meng, X. Tian, C. Wang, L. Xu, X. Zhang, L. Wang and R. Xie, A light-initiated chemical reporter strategy for spatiotemporal labeling of biomolecules, *RSC Chem. Biol.*, 2022, **3**(5), 539–545, DOI: 10.1039/d2cb00072e.
15 Z. Liu, C. Zhang, S. Li, Y. Zhou, F. Lan, X. Zhao, Z. Su, C. Hu, P. Deng and Z. Yu, Light-intersecting Photoclick Reactions for Bioorthogonal Labeling on Single Cells: Dibenzo[b,f][1,4,5]-thiadiazepine-11,11-dioxide as a Photoswitchable Reporter, *Angew. Chem., Int. Ed.*, 2025, **64**(18), e202501936, DOI: 10.1002/anie.202501936.
16 S. Innes-Gold, H. Cheng, L. Liu and A. E. Cohen, Tools for Intersectional Optical and Chemical Tagging on Cell Surfaces, *ACS Chem. Biol.*, 2025, **20**(2), 455–463, DOI: 10.1021/acschembio.4c00756.
17 A. Cook, F. Walterspiel and C. Deo, HaloTag-Based Reporters for Fluorescence Imaging and Biosensing, *ChemBioChem*, 2023, **24**(12), e202300022, DOI: 10.1002/cbic.202300022.
18 G. V. Los, L. P. Encell, M. G. McDougall, D. D. Hartzell, N. Karassina, C. Zimprich, M. G. Wood, R. Learish, R. F. Ohana and M. Urh, *et al.*, HaloTag: A Novel Protein Labeling Technology for Cell Imaging and Protein Analysis, *ACS Chem. Biol.*, 2008, **3**, 373–382.
19 E. F. Ullman and W. A. Henderson, Photochemical Valence Tautomerization Mechanism of Indenone and Cyclopentadienone Oxides. III, *J. Am. Chem. Soc.*, 2002, **86**(22), 5050–5051, DOI: 10.1021/ja01076a095.
20 X. Xie, F. Hu, Y. Zhou, Z. Liu, X. Shen, J. Fu, X. Zhao and Z. Yu, Photoswitchable Oxidopyrylium Ylide for Photoclick Reaction with High Spatiotemporal Precision: A Dynamic Switching Strategy to Compensate for Molecular Diffusion, *Angew. Chem., Int. Ed.*, 2023, **62**(17), e202300034, DOI: 10.1002/anie.202300034.
21 V. Singh, U. Murali Krishna, Vikrant and G. K. Trivedi, Cycloaddition of oxidopyrylium species in organic synthesis, *Tetrahedron*, 2008, **64**(16), 3405–3428, DOI: 10.1016/j.tet.2008.01.049.
22 A. Gautier, A. Juillerat, C. Heinis, I. R. Correa Jr, M. Kindermann, F. Beaufils and K. Johnsson, An engineered protein tag for multiprotein labeling in living cells, *Chem. Biol.*, 2008, **15**(2), 128–136, DOI: 10.1016/j.chembiol.2008.01.007.
23 J. Wilhelm, S. Kuhn, M. Tarnawski, G. Gotthard, J. Tunnermann, T. Tanzer, J. Karpenko, N. Mertes, L. Xue and U. Uhrig, *et al.*, Kinetic and Structural Characterization of the Self-Labeling Protein Tags HaloTag7, SNAP-tag, and CLIP-tag, *Biochemistry*, 2021, **60**(33), 2560–2575, DOI: 10.1021/acs.biochem.1c00258.
24 I. R. Corrêa Jr, B. Baker, A. Zhang, L. Sun, C. R. Provost, G. Lukinavičius, L. Reymond, K. Johnsson and M.-Q. Xu, Substrates for improved live-cell fluorescence labeling of SNAP-tag, *Curr. Pharm. Des.*, 2013, **19**, 5414–5420.
25 F. Walterspiel, B. Ugarte-Uribe, J. Weidenhausen, M. Vincent, K. K. Narayanasamy, A. Dimitriadi, A. U. M. Khan, M. Fritsch, C. W. Muller and T. Zimmermann, *et al.*, A Photoswitchable HaloTag for Spatiotemporal Control of Fluorescence in Living Cells, *Angew. Chem., Int. Ed.*, 2025, e202424955, DOI: 10.1002/anie.202424955.
26 J. B. Grimm, B. P. English, J. Chen, J. P. Slaughter, Z. Zhang, A. Revyakin, R. Patel, J. J. Macklin, D. Normanno and R. H. Singer, *et al.*, A general method to improve fluorophores for live-cell and single-molecule microscopy, *Nat. Methods*, 2015, **12**(3), 244–250, DOI: 10.1038/nmeth.3256, 243 p following 250.
27 D. Si, Q. Li, Y. Bao, J. Zhang and L. Wang, Fluorogenic and Cell-Permeable Rhodamine Dyes for High-Contrast Live-Cell Protein Labeling in Bioimaging and Biosensing, *Angew. Chem., Int. Ed.*, 2023, **62**(45), e202307641, DOI: 10.1002/anie.202307641.
28 C. G. Parker and M. R. Pratt, Click Chemistry in Proteomic Investigations, *Cell*, 2020, **180**(4), 605–632, DOI: 10.1016/j.cell.2020.01.025.
29 E. Kozma and P. Kele, Bioorthogonal Reactions in Bioimaging, *Top. Curr. Chem.*, 2024, **382**(1), 7, DOI: 10.1007/s41061-024-00452-1.